PROCEEDINGS, 49th Workshop on Geothermal Reservoir Engineering
Stanford University, Stanford, California, February 12-14, 2024
SGP-TR-227

Assessment of the Impacts of Multi-Scale Sedimentological Heterogeneity on Low-Enthalpy Geothermal Energy Production

Kiley Baird, Sebastian Geiger, Gary J. Hampson, Carl Jacquemyn, Matthew D. Jackson, Dmytro Petrovskyy, Daniel Arnold, and Florian Doster

Energy Academy, Heriot-Watt University, Currie EH14 4AP

Ksb2001@hw.ac.uk

Keywords: Rapid Reservoir Modelling, geological modelling, geological uncertainty, geothermal reservoir simulation

ABSTRACT

With the increasing demand for sustainable energy solutions to achieve net-zero emission targets, low-enthalpy geothermal developments have emerged as pivotal contributors to the decarbonization of the heating and cooling sector. Geological uncertainty, which is inherent to all subsurface reservoirs but particularly prominent in geothermal systems due to limited data availability and complex subsurface conditions, directly affects resource assessment, risk mitigation and drilling operations.

In order to address geological uncertainty, a robust and efficient modelling and simulation approach that analyses a wide range of geological heterogeneity is needed. This allows us to analyze the extent to which multi-scale and hierarchical geological heterogeneities impact heat and mass transport in low-enthalpy geothermal reservoirs, which remains an area of limited understanding. Our study hence aims to conduct a qualitative assessment of the scale at which geological heterogeneity has significant implications on the expected heat flow rates in a low-enthalpy geothermal system situated in a shallow-marine sedimentary reservoir.

Utilizing open-access 3D geological models of shallow marine sequences previously designed using the Rapid Reservoir Modelling (RRM) software, we simulate heat and fluid flow and the associated well behavior, considering 1 km spaced geothermal doublets. The geological models capture a wide range of multi-scale and hierarchical sedimentological heterogeneity, varying from centimeters (e.g., bioturbation) to kilometers in length (e.g., geometry of the shoreline). Different well placements were screened efficiently using inbuilt flow diagnostics in RRM prior to performing time-consuming heat and fluid flow simulations using a commercial simulator.

Our results show which length-scales of heterogeneity have a more profound effect on low-enthalpy geothermal energy production in shallow marine deposits, and which length-scales can be excluded in reservoir modelling studies. We highlight the importance of using geologically realistic models to capture geological uncertainty in a comprehensive way. We recommend that an efficient screening approach could be beneficial to analyze which sedimentological heterogeneities impact the behavior of a geothermal system most, and which hence need to be characterized with due care so that they can be included reliably in reservoir simulation studies.

1. INTRODUCTION

Geothermal energy recovery from low-enthalpy reservoirs is expected to play a vital role in achieving net-zero targets. For example, the European Union has set the target that 25% of space heating should be covered by geothermal energy (Geothermal IWG, 2023). Hot sedimentary aquifers (HSA) have hence become a focus of attention as they are more prevalent than traditional geothermal systems that are associated with volcanic activity and pose fewer technical difficulties than engineered geothermal systems (Wolff-Boenisch and Evans, 2013). While the global installed capacity for direct-use geothermal continues to increase (Lund and Toth, 2021), geothermal energy only covers a very minor part of the total global energy demand (Energy Institute, 2023; Smil, 2017) and global targets for scaling up geothermal energy are at risk (IRENA, 2022). One major contributing factor to these challenges are the tight economic margins and low return on investment of geothermal energy developments. This in turn implies that the relative cost of collecting subsurface data is high compared to traditional hydrocarbon projects (Saeid et al., 2021). As a result, the geological uncertainty inherent to geothermal reservoirs is often exacerbated, which impacts our ability to forecast the efficiency of heat extraction and economic viability of a geothermal development. Accurate modelling which involves a realistic assessment of the different geological concepts that could represent a geothermal reservoir is therefore crucial to developing a geothermal resource in a safe, sustainable, and viable way (Witter et al., 2019).

It is generally well-understood that geological heterogeneity impacts the longevity and performance of a geothermal system (e.g., Blank et al., 2021; Schulte et al., 2020; Willems and Nick, 2019; Willems et al., 2017a, b). Several studies have specifically analyzed how different types of heterogeneity affect low-enthalpy geothermal energy production. Babei and Nick (2019) investigated heat flow in low-enthalpy aquifers with different degrees of permeability heterogeneity and geometric complexity. They found that the performance of geothermal systems is affected most by permeability distributions with strong spatial correlations and anisotropy but did not consider the impact of geologically realistic, hierarchical, and multi-scale reservoir heterogeneities. Crooijmans et al. (2016) investigated the lifetime and heat recovery as a function of net-to-gross (N/G) ratio in reservoirs. They found that geological heterogeneities based on a random facies generator as opposed to a process-based modelling approach overestimate the lifetimes of the reservoirs, therefore highlighting the need to represent geological heterogeneity in a consistent and geometrically realistic way for reliable forecasts of geothermal reservoir performance. Major et al. (2023) analyzed heat flow in a geothermal reservoir considering process-based, stochastic, and deterministic

methods to model layered clastic reservoir systems. They found that well-designed stochastic models can estimate breakthrough time and production temperature decline for high N/G ratios and that using only reservoir and non-reservoir units may be sufficient in modelling low-enthalpy geothermal reservoirs. However, the investigated models had N/G ratios around 85% and more research is necessary to identify the difference between stochastic and process-based modelling methods when N/G is lower. These studies all show that not only geological impacts reservoir performance but also the way geological heterogeneity is represented in a reservoir model. In other words, a consistent way to model heterogeneity of geothermal reservoirs is needed. What is less well understood in this regard is which length-scale and type of a geobody within the overall reservoir architecture needs to be captured in a reservoir model and if the length-scale and type of the geobody vary as a function of permeability contrast.

The aim of this paper is therefore to provide new insights into how different length-scales of heterogeneity in a geological model affect geothermal production forecasts within deep HSA. As parasequences of shallow-marine origin are one of the main depositional sequences hosting subsurface reservoirs with good reservoir quality (Colombera and Mountney, 2020) and are often found in sedimentary basins that have excellent conditions for hosting aquifer systems that can be utilized for geothermal production (Moeck, 2014), our study focuses on heterogeneities inherent to shallow marine sequences. We use permeability as the key property representing inter-facies heterogeneity as the variance of facies-specific heat capacity is usually small and has a negligible impact on reservoir performance (Zhang et al., 2021) while variability in facies-specific thermal conductivity can be upscaled effectively (Rühaak et al., 2015). We use selected models of shallow marine sequences that are part of a larger open-access reservoir model ensemble that was created by Jackson et al (2022) with the open-source Rapid Reservoir Modelling (RRM) software (Jacquemyn et al., 2021; Petrovskyy et al., 2023). These models were specifically designed to explore the hierarchy of heterogeneity observed in well, core, seismic and outcrop analogue data (Jackson et al., 2022), and have permeability variations from 10^{-3} mD to 10^{3} mD. This model ensemble therefore allows us to investigate how a broad and geologically consistent range of length-scales and heterogeneities impact heat flow in low-enthalpy geothermal energy systems. In this study we further discuss an efficient workflow that utilizes geologically consistent models to capture a wide range of geological scenarios within a data-poor environment to understand the overarching scope of the study area, moving away from a more traditional approach that is centered around a single base case model (Witter et al., 2019; Bentley, 2016).

2. METHODS

2.1 Geological models

We use two geological scenarios for the Johansen and Cook formations (Jackson et al. 2022). These scenarios were represented in RRM and the resulting two models contain three different sets of petrophysical values for each facies, resulting in six individual models that are considered for flow simulations and sensitivity analyses in our study. Although the shallow-marine sandstones of the Johansen and Cook formations are located offshore Norway (Sundal et al 2013; 2016; Meneguolo et al 2022), they contain many of the heterogeneities that are typically encountered in the same environments of deposition located onshore and are hence relevant to geothermal reservoirs. Each model contains four facies associations (FA), depicting mixed fluvial, tidal and wave-dominated depositional environments (Figure 1). Using experimental design techniques, Jackson et al (2022) originally created an ensemble of geological models that captures variations of eight individual sedimentological heterogeneities, which are classified as large (from 10 m – 3 km) and small below 10 m) (Table 1). For example, the planform geometry, the largest sedimentological heterogeneity, represents the overall architecture of the facies associations in the models and is explicitly represented (Figure 2). In a low setting for this geological feature, the model is characterized by a paleoseaward (east to west), tidal sand deposit, creating a linear-to-arcuate deltaic shoreline that progressively becomes more wave-dominated over time (Jackson et al., 2022). In contrast, the high setting for planform geometry is composed of subaqueous clinoforms fed by the wave-dominated deposition of sand parallel to the shoreline (southward), creating a more complex delta architecture (Jackson et al., 2022). The small-scale mudstone drapes or bioturbation within individual parasquences are modelled by changing k_v/k_h ratios and permeability averages for the corresponding FA, respectively (Tables 1 and 2). The porosity and permeability values (Table 2) were derived from core samples (Jackson et al., 2022). Two additional model scenarios are considered here where the overall permeability is reduced by a factor 10 to test how reduced permeability affects the overall reservoir behavior. Table 3 summarizes the properties of each individual model. For a more detailed background of the geological context, subsurface data, and modelling methodology, please refer to Jackson et al (2022). Each model is 2500 m x 3000 m x 200 m in size with a grid resolution of 101 x 101 x 71 grid blocks. The reservoir is assumed to be at a depth of 2.5 km with initial temperatures and pressure set to 80 °C and 250 bars, respectively, throughout the entire model. Heat capacity is set to 2.347×10^{6} J/m^3 °C and the thermal conductivity is set to 1.5×10^{5} J/(m day °C) for all FAs.

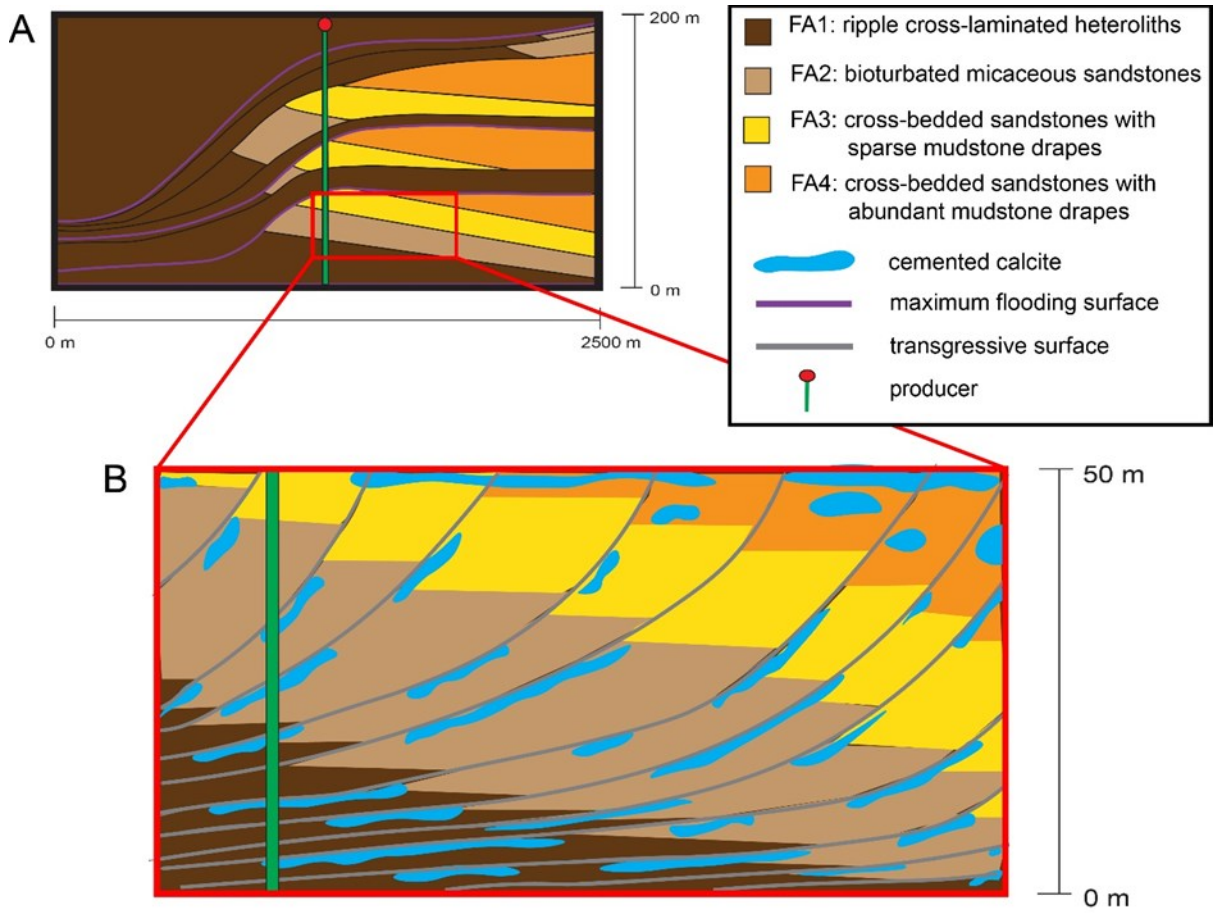

Figure 1: Cross-sectional view of facies associations (FA) at different scales: A) regressive-transgressive tongues of vertically stacked successions (clinoform sets), and B) a single clinoform set at a higher resolution detailing the interfingering of facies associations and calcite cementation along transgressive surfaces (redrawn from Jackson et al., 2022).

Table 1: Small- and large-scale sedimentological heterogeneities in the reservoir models and their low or high settings.

Scale of heterogeneity	Sedimentological heterogeneity	Low setting	High setting
Small	Bioturbation intensity	Less bioturbated; kh = arithmetic mean (Table 2)	More bioturbated; kh = geometric mean (Table 2)
	Mudstone drape continuity and extent in heterolithic cross-bedded sandstones (FA3 and FA4 only)	Sandstone proportion = 1.0; kv/ kh ratio = 1.0	Sandstone proportion = 0.97; kv/ kh ratio = 0.1
	Mean lateral extent of carbonate-cemented concretions in between transgressive surfaces	5.1 m	32.7 m
	Mean vertical spacing of carbonate-cemented concretions in between transgressive surfaces	1 m	6 m

Large	Dip extent of facies interfingering down clinoforms	Small (10-150 m)	Large (100-250 m)
	Lateral continuity of carbonate-cemented concretions along transgressive surfaces and maximum flooding surfaces	100 m	1000 m
	Clinoform dip	Gentle (1°)	Steep (3°)
	Planform geometry	Westward-prograding, arcuate delta	Southward-deflected, elongate delta

Table 2: Horizontal permeability values for each facies association (FA).

k_h (mD)		
Facies association	Arithmetic mean	Geometric mean
FA1	2.0	0.25
FA2	130	80
FA3	1100	490
FA4	2200	1300

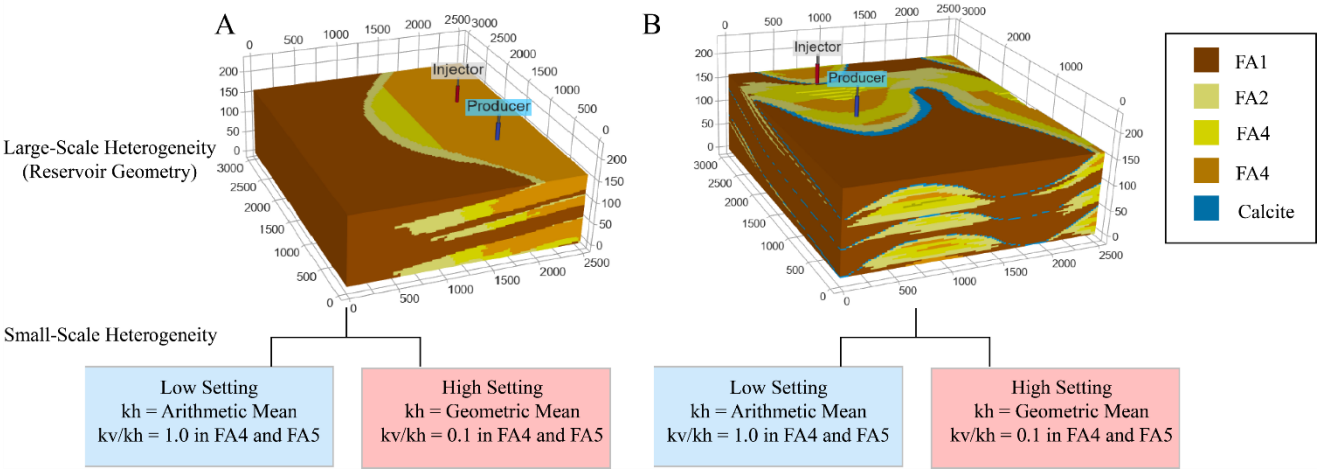

Figure 2: Geometries and parameters for small- and large-scale heterogeneities, given either A) a westward prograding arcuate delta with gentle clinoform dip, 100 m lateral continuity of carbonate-cemented concretions along transgressive and maximum flooding surfaces, and 10-150 m dip extent of facies interfingering down clinoform surfaces, or B) a southward-deflected elongate delta with steeper clinoform dip, 1000 m lateral continuity of carbonate-cemented concretions along transgressive and maximum flooding surfaces, and 100-250 m dip extent of facies interfingering down clinoform surfaces.

Table 3: Petrophysical values assigned to each facies association (FA) for each of the 6 models.

	Model	1) *low* large-scale; *low* small-scale	2) *low* large-scale; *high* small-scale	3) *high* large-scale; *high* small-scale	4) *high* large-scale; *low* small-scale	5) *low* large-scale; *high* small scale; permeability	6) *high* large-scale; *high* small scale; permeability

						reduced by factor 10	reduced by factor 10
kh (mD)	FA1	2	0.25	0.25	2	0.025	0.025
	FA2	130	80	80	130	8	8
	FA3	1100	490	490	1100	49	49
	FA4	2200	1300	1300	2200	130	130
	Calcite	-	-	0.1	0.1	-	0.1
kv (mD)	FA1	0.2	0.025	0.025	0.2	0.0025	0.0025
	FA2	13	8	8	13	0.8	0.8
	FA3	110	49	49	110	4.9	4.9
	FA4	220	130	130	220	13	13
	Calcite	-	-	0.1	0.1	-	0.1
Porosity (%)	FA1	14	14	14	14	14	14
	FA2	27	27	27	27	27	27
	FA3	24	24	24	24	24	24
	FA4	25	25	25	25	25	25
	Calcite	-	-	5	5	-	5

2.2 Dynamic reservoir simulation

Geothermal production was simulated for 60 years using a commercial simulator (STARS by CMG Ltd.). Fluid properties (i.e., density, viscosity, and heat capacity) are computed as a function of pressure and temperature in the simulator, assuming that the fluid is pure water. The injection and production wells are set 1 km apart and target the permeable facies in the given reservoir geometry (Figure 2). We run two sets of simulations with the wells orientated north to south (N-S) or west to east (W-E). Injection and production rates are set to a constant 100 l/s with secondary bottom hole pressure (BHP) constraints of 300 bars and 200 bars, respectively. Initial sensitivity runs show that these BHP constraints are usually not reached. Reinjection temperature is set to 30°C. Both wells are perforated throughout the entire depth of the model.

2.2.1 Auxiliary equations

We define the geothermal capacity E_n [MW_{TH}] as the difference between the gross production energy E_g and the pump energy E_p given by

$$E_n = E_g - E_p. \quad (1)$$

E_g can be directly obtained from the simulator as

$$E_g = \sum_{i=1}^{n} Q_i \Delta t_i \rho_{f,i} C_{f,i} \left(T_{prod,i} - T_{inj}\right), \quad (2)$$

where Q_i is well flow rate [l/s], Δt_i is the timestep [s], ρ_f is the fluid density [kg/m^3], C_f is the fluid's specific heat capacity [J/m°C], and T the temperature [°C]. The pump energy E_p is calculated using the BHP of the injection well P_i and production well P_p over time given by

$$E_p = \sum_{i}^{n} Q_i \Delta t_i \left(P_i - P_p\right). \quad (3)$$

3. RESULTS

3.1 Production energy

The cumulative production energy E_g (Eq. 2) is affected by the large-scale heterogeneity as well as the orientation of the injector producer pair (Figure 3). Models with the high setting for the large-scale heterogeneities, such as a southward deflected elongate delta and steeper clinoform dip (Models 1, 2, and 5), yield higher E_g for both well orientations (E_g from 3.46x10^{16} J to 3.69x10^{16} J) than models with low

setting, i.e. those with a westward prograding arcuate delta and less and lower angle clinoform dip (Models 3, 4, and 6) (E_g from 3.25x10^{16} to 3.34x10^{16} J). This represents a 5% increase in E_g for Models 1,2, and 5 compared to Models 3, 4, and 6 for N-S orientated wells, and 10% increase in E_g for Models 1, 2, and 5 compared to Models 3, 4, and 6 for W-E orientated wells. E_g calculated for Models 1, 2 and 5 is also more sensitive to well orientations (E_g changes by 1.38x10^{15} to 1.77x10^{15} J or 4 to 5%) compared to E_g calculated for Models 3, 4 and 6 for the different well orientations (E_g changes by 2.27x10^{14} to 3.75x10^{14} J or approximately 1%). In other words, Models 1, 2, and 5 show consistently higher E_g but also a wider distribution in E_g compared to Models 3, 4, and 5. Reducing the overall permeabilities by a factor of 10 (Models 5 and 6) was observed to have minimal impact on the E_g as long as the well orientation is the same. This implies that at least some of the impact of geological uncertainty can be mitigated if the well orientation is chosen properly, but this in turn requires us to model and explore different reservoir geometries adequately.

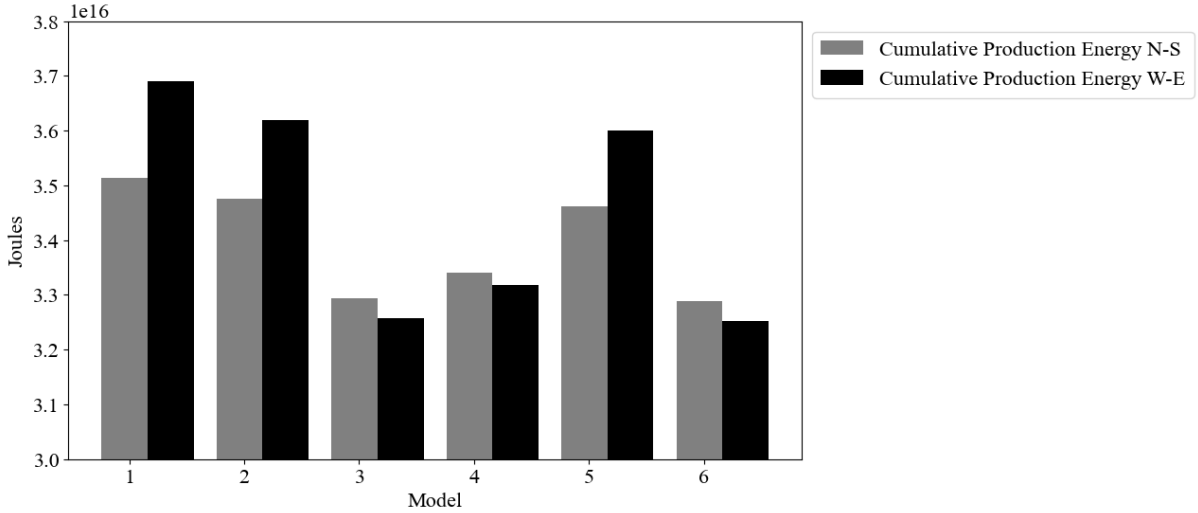

Figure 3: Cumulative energy produced over 60 years of simulation for each model and well orientation.

Where the models have the same setting for the large-scale geological heterogeneities and well orientation but different small-scale heterogeneities (e.g. Models 1 and 2 for N-S and W-E orientated wells or Models 3 and 4 for N-S and W-E orientated wells), little difference in E_g is observed (≤ %2). Models 5 and 6 with the reduced overall permeability also show very little difference in E_g.

3.2 Pump energy

The approximated pump energy E_p (Eq. 3) is more variable across all models, with values ranging from 9.4x10^{13} J in model 1 (N-S well orientation) to 5.2x10^{15} J in model 6 (W-E well orientation) (Figure 4). This is not surprising because the well controls aim to maintain the same flow rates, so BHP pressures need to be adjusted to achieve the target flow rates for the given reservoir heterogeneity. This is particularly apparent for Models 5 and 6 with the reduced permeability; here E_p is one magnitude larger than for the other models, with the highest E_p observed for the W-E orientated wells. In contrast to E_g, changing the setting for the small-scale heterogeneity also has noticeable impacts on E_p. Models containing the same large-scale heterogeneities, but different small-scale heterogeneities (e.g., Models 1 and 2 and Models 3 and 4) yield differences in E_p of 55 to 71%, with the exception of Models 5 and 6. Changing the well orientation from N-S to W-E increases the E_p by 60 to 85% for all six models.

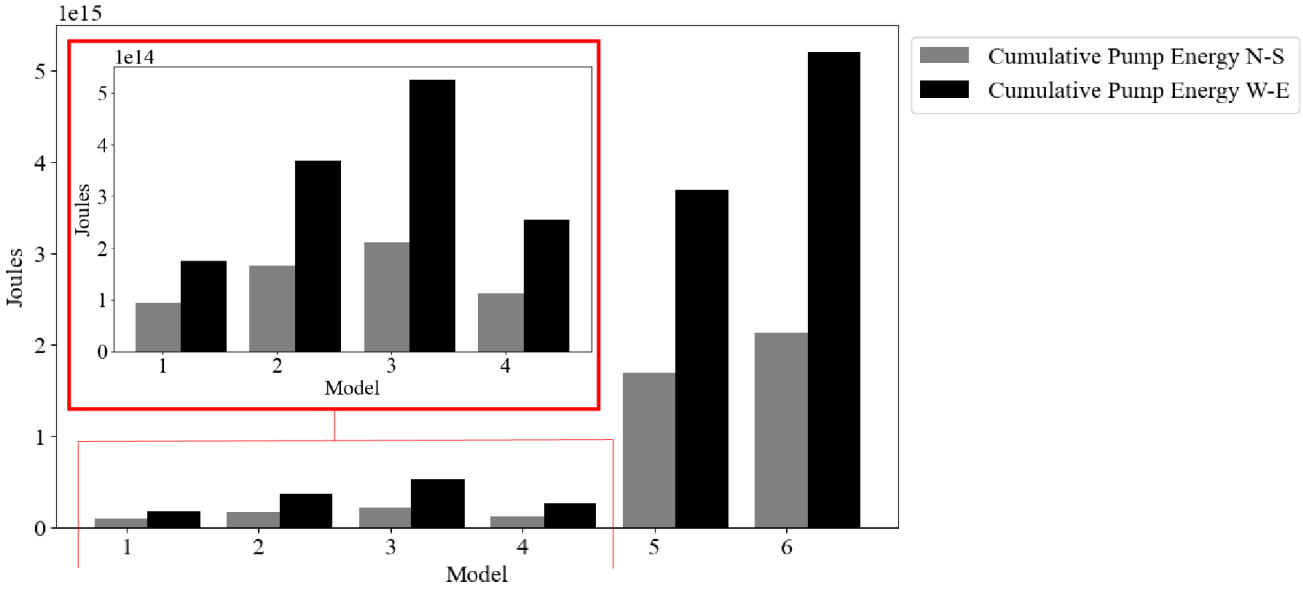

Figure 4: Cumulative energy required by the pumps over the 60-year simulation period for all models.

3.3 Geothermal capacity

Geothermal capacity estimates are a composite of the cumulative energy produced and the energy losses from the pump (Eq. 1). E_n ranges from 14 to 19 MW_{TH} with highest estimates observed for Models 1 and 2 (Figure 5), which are characterised by a westward-prograding arcuate delta, gentle clinoform dip, 100 m lateral continuity of carbonate-cemented concretions and a 10 to 150 m dip extent of facies interfingering down clinoform surfaces (low settings for large-scale heterogeneities). E_n for Models 4 and 5 varies only by 0.5 MW_{TH} for both well orientations. Overall, well orientations have a surprisingly minor impact on E_n for Models 1 to 5, but there is a significant reduction in E_n where wells are orientated W-E not N-S in Model 6. Further, decreasing the permeability by a factor of 10 reduces E_n by 0.88 to 1.85 MW_{TH} between Models 2 and 5 and 1 to 4.5 MW_{TH} between Models 3 and 6.

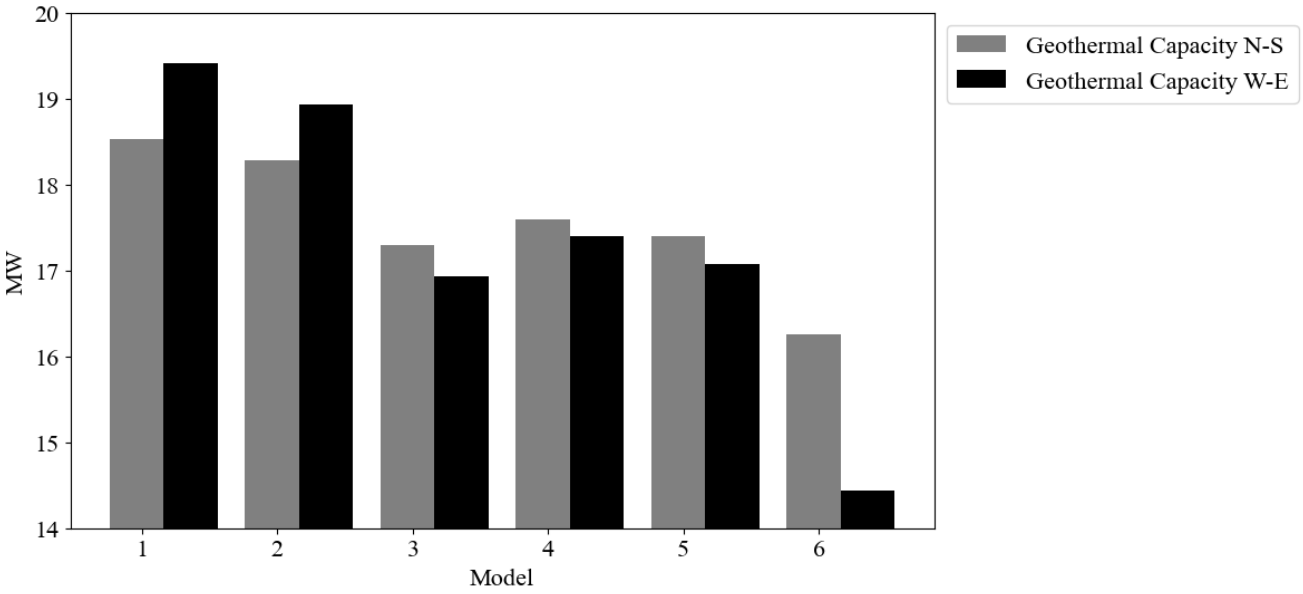

Figure 5: Total geothermal capacity for each model given 60 years of production.

4. DISCUSSION

4.1 Impact of heterogeneity scales on geothermal capacity

Our results show that the overall geothermal capacity estimates are a balance between the production rates, controlled predominantly by the size of the drainage area around the production well, as well as the energy required to pump fluids, controlled predominantly by the

reservoir pressure and hence reservoir connectivity and permeability. Where models have a westward-prograding arcuate delta with a gentle clinoform dip, 100 m lateral continuity of carbonate-cemented concretions, and 10 to 150 m dip extent of facies interfingering down clinoforms (Models 1, 2, and 5) we observe higher cumulative production values. In Models 1 and 2, this therefore contributes to the highest estimates for geothermal capacity; however, the geothermal capacity for Model 5 is reduced by the large pump energy required to provide sufficient flow rates, which yields results similar to models with high settings for the large-scale heterogeneities, i.e. the models that have a southward-deflected elongate delta with steeper clinoform dip, 1000 m lateral continuity of carbonate-cemented concretions, and 100 to 150 m dip extent of facies interfingering down transgressive surfaces (Models 3 and 4). While Models 1 and 2 have varying settings for small-scale heterogeneity (e.g., less or more bioturbated; sandstone proportion = 1.0 or 0.1; 5.1 m or 32.7 m lateral extent of carbonate-cemented concretions; 1 m or 6 m mean vertical spacing of carbonate-cemented concretions), little differences in geothermal capacity (≤ 0.5 MW$_{TH}$) are observed. From this we deduce that the large-scale heterogeneities either control channelling or provide baffles that reduce the drainage volume around the producer, both of which impact reservoir performance in different ways for a given the layout of the well pair. Similar observations were also made by Liu et al., (2019) and Willems et al. (2017a, b). For example, in models with westward-prograding arcuate deltas (Models 1, 2, and 5) and well pairs orientated N-S, we observe that the production well drains the most permeable facies (FA4), both in the direction of the injector and to the south of the producer, creating a large drainage region (Figure 6). Where a southward-deflected elongate delta is present, flow towards the production well is reduced due to the pinch out geometries that restrict flow from the southern part of the reservoir (Figure 6). In contrast to the observations of Babaei and Nick (2019) discussed above, we observe that models with different permeability anisotropy have similar preferential flow paths between injector and producer, yet the area of the accessed drainage volume drives the inflow of colder fluids and reduces the produced energy. Well placement therefore can be manipulated to ensure that the producer has access to a large part of the drainage area, further highlighting the potential for well optimization under geological uncertainty during geothermal developments (Babaei et al, 2022; Daniilidis et al., 2021; Schulte et al., 2020) but also indicating that such robust uncertainty methods need to capture the full range of large-scale reservoir architectures.

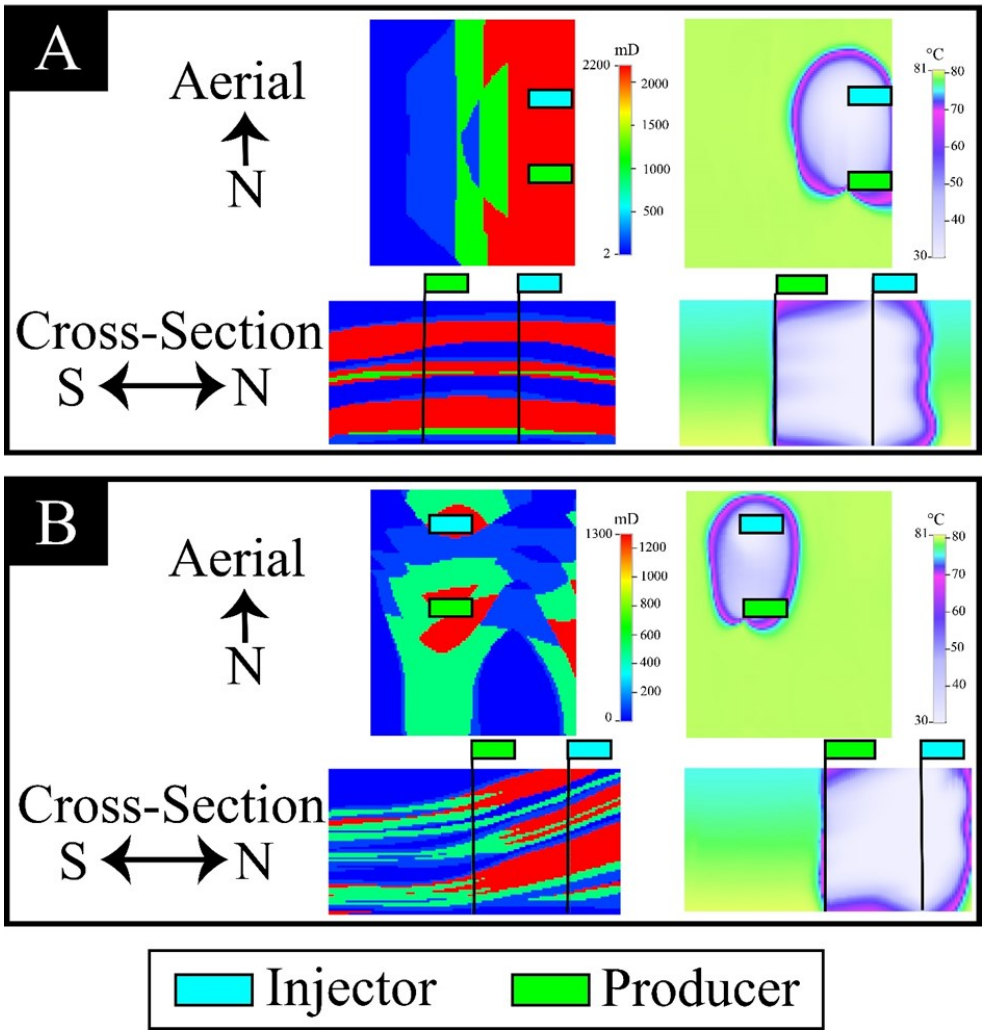

Figure 6: Aerial and cross-sectional views of k_h (mD) and temperature (°C) after 60 years of production for: A) Model 1 with low-setting for small- and large-scale heterogeneity, and B) Model 3 with high-setting for small- and large-scale heterogeneity.

The small-scale heterogeneities, such as bioturbation intensity and mudstone drape continuity, that are reflected in the permeability values of the facies in our models have a larger effect on the pump energy losses than the large-scale heterogeneities. As noted above, the variation

in pump energy is a direct consequence of the well controls which aim to maintain constant flow rates, hence increasing the pressure gradient if baffles, pinch outs, or lower-permeability facies are present. Further, we have perforated the entire depth of the wells, potentially causing discrepancies where impermeable facies are penetrated. This is particularly visible in Models 5 and 6 where the permeability of all FAs has been reduced by a factor of 10. Still, the overall geothermal capacity estimate of Model 5 (17.40 MW_{TH} for N-S orientated wells and 17.08 MW_{TH} for W-E orientated wells) is similar to Model 4 (17.60 MW_{TH} for N-S orientated wells and 17.40 MW_{TH} for W-E orientated wells) but higher than Model 3 (17.30 MW_{TH} for N-S orientated wells and 16.93 MW_{TH} for W-E orientated wells). As we reduce the permeability in Model 5, we begin to reach the point in which pump energy has a more noticeable effect on overall geothermal capacity, resulting in geothermal capacity estimates that are similar to models with more complex planform geometry. The cumulative energy produced is one to three orders of magnitude larger than the estimated energy needed operate the pumps over the 60-year simulation period. Hence the overall geothermal capacity is still dominated by the produced energy, although the variability in pump energy leads to subtle variations in geothermal capacity between the individual models. This picture would likely change if the flow rates at the wells was to be increased even further such that the BHP constrains for the injector and producer are reached and the production rate needs to be reduced more drastically for some models. For the models analysed here, the reservoir architecture and reservoir permeability appear to be high enough to provide reasonable flow rates for several decades. Overall, models with low settings for large-scale heterogeneities (i.e., westward prograding arcuate delta and less and lower angle clinoform dip) that do not have reduced overall permeability represent the best geological scenario for geothermal energy production.

So far, we only consider a subset of the entire reservoir model ensemble of Jackson et al. (2022) that grouped sedimentological heterogeneities into large-scale and small-scale. Hence we are unable to differentiate the effects of each individual sedimentological heterogeneity on the geothermal capacity. Further work will therefore deploy an experimental design similar to that of Jackson et al. (2022) to identify the impact of the full range of geological heterogeneities and length-scales encapsulated in the full model ensemble. This will provide an in-depth sensitivity analysis that provides a detailed ranking of the specific geological structures or petrophysical characteristics that have the largest impact on geothermal capacity in shallow marine sequences. One of the major advantages of RRM is that it allows us to create large model ensembles that capture different scales of geological heterogeneities in a geologically consistent way. Together with the flow diagnostics available in RRM, a broad range of geological scenarios can therefore be tested and screened, which allows us to carry out targeted geothermal reservoir modelling and simulation studies that reliably explore the impact of geological heterogeneity on heat flow in the reservoir and geothermal energy production.

5. CONCLUSIONS

In this study we investigated the impact of geological heterogeneities that are typically encountered in shallow marine sequences during geothermal heat production from a hot sedimentary aquifer. Using geological realistic models that captured the wide range of hierarchical and multi-scale sedimentological uncertainties observed in these depositional environments, we were able to identify important controls on geothermal capacity estimates for low-enthalpy geothermal systems. Our results show that

1) Large-scale (km-scale) geological features impact the cumulative production energy by increasing the drainage volume around the production well and hence rely less on the injected fluid to balance reservoir pressures. In this particular geological example, the westward-prograding arcuate delta was a key controlling geological feature that enhanced the heat production rates. Other large-scale features such as pinch outs increase the inflow of colder fluids via preferential flow paths from the injector to the producer and therefore reduce heat production rates.

2) The cumulative pump energy over 60 years for all geological heterogeneities is one to three magnitudes smaller than the cumulative energy produced. Hence the pump energy has a relatively small impact on the overall geothermal capacity for the chosen well controls and reservoir geology. Still, some deviations in geothermal capacity are observed, which are mainly due to the increased pump energy needed to maintain high flow rates in the low-permeability scenarios.

Overall, we conclude that large-scale geological heterogeneity, such as planform geometry or clinoform dip, are key features in shallow marine sediments that need to be characterised properly during initial exploration phase to understand the overall feasibility of a potential low-enthalpy geothermal play. Such features can be visible on 3D seismic data during the exploration phase, and the open source Rapid Reservoir Modelling software provides an excellent environment to quickly rest different geological scenarios of these large-scale features. Once potential geothermal targets have been identified in shallow marine sequences, further reservoir characterisation and modelling effort should be focused on analysing the connectivity of the reservoir bodies (e.g. isotropic permeability found in the westward-prograding arcuate delta as compared to anisotropic permeability caused by pinchout geometries in the southward-deflected elongate delta). Our initial results suggest that we need to characterise and represent these larger-scale features correctly in our models to ensure that we can produce heat safely and sustainably; a follow-up study that will deploy an experimental design approach to capture the full range of geological heterogeneities in shallow marine sequences aims to confirm this. When more detail is needed to answer specific questions on the ideal production parameters and well optimization, additional small-scale details can be added to the reservoir models. This approach can help to reduce the need for overly detailed and complex reservoir modelling and simulations when analysing a potential geothermal play but also highlights the need for getting the key geological features characterised adequately early on.

6. ACKNOWLEDGMENTS

Kiley's PhD is supported by a James Watt Scholarship at Heriot-Watt University. We thank Energi Simulation for further financial support of this study. We also acknowledge CMG Ltd. for access to STARS and the industrial supporters of the RRM Phase 1 and Phase 2 consortia.

References

Babaei, M., Norouzi, A. M., Nick, H. M., and Gluyas, J.: Optimisation of Heat Recovery from Low-Enthalpy Aquifers with Geological Uncertainty Using Surrogate Response Surfaces and Simple Search Algorithms, Sustainable Energy Technologies and Assessments, 49, (2022), 101754.

Babaei, M., and Nick, H. M.: Performance of Low-Enthalpy Geothermal Systems: Interplay of Spatially Correlated Heterogeneity and Well-Doublet Spacings, Applied Energy, 253, (2019), 113569.

Bentley, M.: Modelling for Comfort?, Petroleum Geoscience, 22, (2016), 3-10.

Blank, L., Rioseco, E. M., Caiazzo, A., and Wilbrandt, U.: Modeling, Simulation, and Optimization of Geothermal Energy Production from Hot Sedimentary Aquifers, Computational Geosciences, (2021), 25, 67-104.

Colombera, L. and Mountney, N. P.: On the Geological Significance of Clastic Parasequences, Earth-Science Reviews, 201, (2020), 103062.

Crooijmans, R. A., Willems, C. J. L., Nick, H. M., and Bruhn, D. F.: The Influence of Facies Heterogeneity on th Doublet Performance in Low-Enthalpy Geothermal Sedimentary Reservoirs, Geothermics, 64, (2016), 209-219.

Daniilidis, A., Saeid, S., & Doonechaly, N. G.: The fault plane as the main fluid pathway: Geothermal field development options under subsurface and operational uncertainty, Renewable Energy, 171, (2021), 927–946.

Energy Institute - Statistical Review of World Energy (2023); Smil (2017) – with major processing by Our World in Data: Primary energy from other renewables [dataset]. Energy Institute, Statistical Review of World Energy; Smil, Energy Transitions: Global and National Perspectives [original data].

Geothermal IWG: Implementation Plan, (2023), https://setis.ec.europa.eu/implementing-actions/geothermal_en. [Accessed 20 Jan. 2024].

IRENA: World Energy Transitions Outlook 2022: 1.5°C Pathway, International Renewable Energy Agency, Abu Dhabi, (2022).

Jackson, W. A., Hampson, G. J., Jacquemyn, C., Jackson, M. D., Petrovskyy, D., Geiger, S., Machado Silva, J. D., Judice, S., Rahman, F., and Costa Sousa, M.: A screening Assessment of the Impact of Sedimentological Heterogeneity on CO_2 Migration and Stratigraphic-Baffling Potential: Johansen and Cook Formations, Northern Lights Project, Offshore Norway, International Journal of Greenhouse Gas Control, 120, (2022), 103762.

Jacquemyn, C., Pataki, M. E. H., Hampson, G. J., Jackson, M. D., Petrovskyy, D., Geiger, S., Marques, C. C., Machado Silva., J. D., Judice, S., Rahman, F., and Costa Sousa, M.: Sketch-based Interfaces and Modeling of Stratigraphy and Structure in Three Dimensions, Journal of the Geological Society, 178, (2021).

Liu, G., Pu, H., Zhao, Z., and Liu, Y.: Coupled Thermo-Hydro-Mechanical Modeling on Well Pairs in Heterogeneous Porous Geothermal Reservoirs, Energy, 171, (2019), 631-653.

Lund, J. W., and Toth, A. N.: Direct Utilization of Geothermal Energy 2020 Worldwide Review, Proceedings, World Geothermal Congress 2020+1, Reykjavik, Iceland (2021).

Major, M., Daniilidis, A., Hansen, T. M., Khait, M., and Voskov, D.: Influence of Process-Based, Stochastic and Deterministic Methods for Representing Heterogeneity in Fluvial Geothermal Systems, Geothermics, 109, (2023), 102651.

Meneguolo, R., Sundal, A., Martinius, A. W., Veselovsky, Z., Cullum, A., and Milovanova, E.: Impact of the Lower Jurassic Dunlin Group Depositional Elements on the Aurora CO_2 Storage Site, EL001, Northern North Sea, Norway, International Journal of Greenhouse Gas Control, 119, (2022), 103723.

Moeck, I. S.: Catalogue of Geothermal Play Types Based on Geologic Controls, Renewable and Sustainable Energy Reviews, 37, (2014), 867-882.

Petrovskyy, D., Jacquemyn, C., Geiger, S., Jackson, M. D., Hampson, G. J., Machado Silva, J. D., Judice, S., Rahman, F., and Costa Sousa, M.: Rapid Flow Diagnostics for Prototyping of Reservoir Concepts and Models for Subsurface CO_2 Storage, International Journal of Greenhouse Gas Control, 124, (2023), 103855.

Rühaak, W., Guadagnini, A., Geiger, S., Bär, K., Gu, Y., Aretz, A., Homuth, S., and Sass, I.: Upscaling Thermal Conductivities of Sedimentary Formations for Geothermal Exploration, Geothermics, 58, (2015), 49-61.

Schulte, D. O., Arnold, D., Geiger, S., Demyanov, V., and Sass, I.: Multi-Objective Optimization Under Uncertainty of Geothermal Reservoirs Using Experimental Design-Based Proxy Models, Geothermics, 86, (2020), 101792.

Sundal, A., Nyusten, J. P., Dipvyk, H., Miri, R., and Aagaard, P.: Effects of Geological Heterogeneity on CO_2 Distribution and Migration – A Case Study from the Johansen Formation, Norway, Energy Procedia, 37, (2013), 5046-5054.

Willems, C. J. L., and Nick, H. M.: Towards Optimization of Geothermal Heat Recovery: An Example from the West Netherlands Basin, Applied Energy, 247, (2019)., 582-593.

Willems, C. J. L., Nick, H. M., Donselaar, M. E., Weltje, G. J., and Bruhn, A. F.: On the Connectivity Anisotropy in Fluvial Hot Sedimentary Aquifers and its Influence on Geothermal Doublet Performance, 65, (2017), 222-233.

Willems, C. J. L., Nick, H. M., Weltje, G. J., and Bruhn, D. F.: An Evaluation of Interferences in Heat Production from Low-Enthalpy Geothermal Doublet Systems, Energy, 135, (2017), 500-512.

Witter, J. B., Trainor-Guitton, W. J., and Siler, D. L.: Uncertainty and Risk Evaluation During the Exploration Stage of Geothermal Development: A Review, Geothermics, 78, (2019), 233-242.

Wolff-Boenisch, D., and Evans, K.: Review of Available Fluid Sampling Tools and Sample Recovery Techniques for Groundwater and Unconventional Geothermal Research as Well as Carbon Storage in Deep Sedimentary Aquifers, Journal of Hydrology, 513, (2014), 68-80.

Zhang, C., Zhang, L., Wang, X., Rao, S., Zuo, Y., Huang, R., Gao, P., Song, R. and Wang, Z.: Effects of the Spatial Heterogeneity in Reservoir Parameters on the Heat Extraction Performance Forecast Based on a 3D Thermo-Hydro-Mechanical Coupled Model: A Case Study at the Zhacang Geothermal Field in the Guide Basin, Northeastern Tibetan Plateau, Geothermics, 95, (2021), 102161.